Importance of σ Bonding Electrons for the Accurate Description of Electron Correlation in Graphene

Huihuo Zheng, Yu Gan, Peter Abbamonte, and Lucas K. Wagner

Phys. Rev. Lett. **119**, 166402 — Published 20 October 2017

DOI: 10.1103/PhysRevLett.119.166402

The importance of σ bonding electrons for the accurate description of electron correlation in graphene

Huihuo Zheng, Yu Gan, Peter Abbamonte, and Lucas K. Wagner*
Department of Physics, University of Illinois at Urbana-Champaign, Urbana, Illinois 61801-3080, USA
(Dated: September 7, 2017)

Electron correlation in graphene is unique because of the interplay between the Dirac cone dispersion of π electrons and long range Coulomb interaction. Because of the zero density of states at Fermi level, the random phase approximation predicts no metallic screening at long distance and low energy, so one might expect that graphene should be a poorly screened system. However, empirically graphene is a weakly interacting semimetal, which leads to the question of how electron correlations take place in graphene at different length scales. We address this question by computing the equal time and dynamic structure factor $S(\boldsymbol{q})$ and $S(\boldsymbol{q},\omega)$ of freestanding graphene using *ab-initio* fixed-node diffusion Monte Carlo and the random phase approximation. We find that the σ electrons contribute strongly to $S(\boldsymbol{q},\omega)$ for relevant experimental values of ω even at distances up to around 80 Å. These findings illustrate how the emergent physics from underlying Coulomb interactions results in the observed weakly correlated semimetal.

Graphene has drawn much attention in the last decade because of its unusual electronic and structural properties and its potential applications in electronics [1–8]. Although many electronic properties of graphene can be correctly described in a noninteracting electron picture [8], electron-electron interactions do play a central role in a wide range of phenomena that have been observed in experiments [9]. For example, the reshaping of the Dirac cone was first predicted [10–12] and later observed experimentally [13]. The fractional quantum hall effect has been observed under large magnetic field [14]. Collective plasmon and plasmaron excitation have also been observed [15–18].

Two-dimensional Dirac systems exhibit interesting features due to the influence of Coulomb interactions. The random phase approximation (RPA) predicts a constant dielectric constant as the frequency and wavelength approach zero. This is in contrast to normal metals, where charge carriers and impurities are highly screened by the Fermi sea through the formation of virtual electron-hole pairs according to RPA [19]. All systems with linear dispersion, including Weyl semimetals [20–23] and surface states of topological insulators [24–26] require similar consideration. The electronic response in graphene is thus interesting not only for itself, but for a broad class of materials currently under study.

In recent years, it has become possible to obtain very high resolution inelastic X-ray scattering (IXS) experiments on graphite [27, 28], which were then analyzed to obtain information about the graphene planes. These experiments directly probe the dynamical structure factor $S(\boldsymbol{q},\omega)$, which allows for a detailed look at the electron correlations. The main purpose of these experiments was to investigate the role of screening at long wavelengths, and particularly whether the RPA obtains an accurate representation of the physics at long range. While these studies obtained unprecedented details about the low-energy charge excitations, their interpretation is challenging because of limited experimental resolution and uncertainties about the reference for the RPA; whether the σ bonding electrons are included or not, and the choice of the underlying theory, have large effects on the result [29]. For small enough wavevector q and small enough frequency ω, the effect of σ electrons should be negligible, but it is unclear whether the experiments have reached that regime.

In this manuscript, we address both the question of the suitability of RPA perturbation theory and the effect of σ electrons by applying highly accurate first-principles diffusion quantum Monte Carlo (DMC) to graphene and a series of related planar honeycomb systems. DMC is a non-perturbative method with minimal approximations [30–32] and explicit representation of the electron-electron interactions. It has been shown to be a highly accurate method on both molecular systems and solids [30–38]. We compute the structure factor $S(\boldsymbol{q})$ which gives information about the long-range density-density correlations in the material and compare it directly to X-ray data, obtaining agreement within the experimental error bars. We find that the σ bonding electrons are surprisingly important even at the longest range accessible to experiment. In addition, if the RPA is performed including the σ electrons from a DFT reference, it is in good agreement with the experimental data, although the absolute peak locations do depend on the reference as noted previously [29].

The structure factor $S(\boldsymbol{q})$ is a measure of the equal-time charge-charge correlations of the system, defined as

$$S(\boldsymbol{q}) \equiv \frac{1}{N}\langle \rho_{-\boldsymbol{q}}\rho_{\boldsymbol{q}}\rangle, \tag{1}$$

where N is the number of electrons in the system, and $\rho_{\boldsymbol{q}} = e^{i\boldsymbol{q}\cdot\hat{\boldsymbol{r}}}$ is the density operator in reciprocal space. $S(\boldsymbol{q})$ is directly related to the Coulomb interactions of the system [39],

$$V = \frac{e^2}{4\pi^2}\int d\boldsymbol{q}\frac{S(\boldsymbol{q})-1}{q^2}, \tag{2}$$

where V is the Coulomb energy per particle. $S(\boldsymbol{q})$ is the integral of the dynamic structure factor $S(\boldsymbol{q},\omega)$ over frequency domain:

$$S(\boldsymbol{q}) = \int_0^\infty \frac{d\omega}{2\pi} S(\boldsymbol{q},\omega) = \frac{\hbar \boldsymbol{q}^2}{2m} \frac{\int_0^\infty d\omega S(\boldsymbol{q},\omega)}{\int_0^\infty d\omega \omega S(\boldsymbol{q},\omega)}. \quad (3)$$

Here we have applied the f-sum rule [19]. $S(\boldsymbol{q},\omega)$ describes the dielectric response of the system [19]. It can be measured through IXS experiment [27, 28], and can be computed using RPA [19, 40].

The first-principles calculations were performed as follows. DFT calculations were first performed using the CRYSTAL package [41] with the Perdew-Burke-Ernzerhof (PBE) exchange and correlation functional [42]. The simulations were performed on a 16×16 supercell including 512 atoms. Burkatzki-Filippi-Dolg (BFD) pseudopotentials [43, 44] were used to remove the core electrons. The result of the DFT calculations was a Slater determinant made of Kohn-Sham orbitals. The Slater determinant was then multiplied by a Jastrow correlation factor and optimized using variance optimization [30]. DMC calculations were performed at Γ point using the QWalk package [33] to obtain $S(\boldsymbol{q})$. RPA calculations were performed using the GPAW package [45, 46] to obtain $S(\boldsymbol{q},\omega)$. The Hubbard model was solved by auxiliary-field quantum Monte Carlo method (AFQMC) using the QUEST package [47].

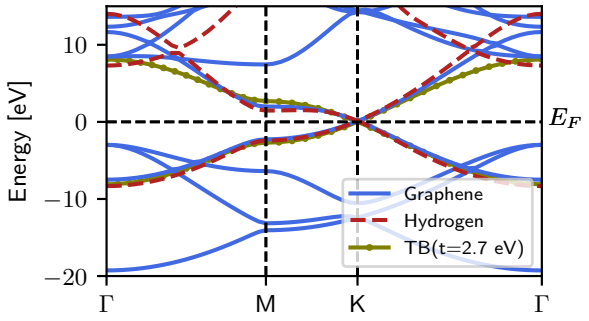

FIG. 1. Band structure of graphene, hydrogen and the tight-binding model (with nearest-neighbor hopping $t = 2.7$eV). Graphene and hydrogen band structures are from DFT calculation with PBE functional.

In order to disentangle different contributions to $S(\boldsymbol{q},\omega)$ from the π and σ electrons in graphene, we compared $S(\boldsymbol{q})$ of the five systems listed in Table I. All systems have similar low energy band structure (Fig. 1), but differ in the presence or absence of the σ electrons, and in the interaction between electrons. The s orbital of the hydrogen system (with the same lattice constant $a = 2.46$ Å as graphene) has almost the same dispersion as the π orbital in graphene. The similarity between these two systems provides a way to understand the behavior of π electrons in graphene in the absence of σ electrons while still retaining a $1/r$ interaction. Graphene and the hydrogen model system are studied using DMC and RPA. The tight-binding model (t=2.7eV) is studied using RPA with $1/r$ interactions. $S(\boldsymbol{q})$ is obtained by integration of $S(\boldsymbol{q},\omega)$ according to Eq. (3).

TABLE I. Systems/models investigated

system/model	electrons	method
Graphene (G): $a = 2.46$ Å	σ & π	DMC, S-J[a], RPA
π-only graphene (G_π)	π	S-J[b]
Hydrogen (H): $a = 2.46$ Å	s	DMC, RPA
Tight-binding (TB): $t = 2.7$ eV	π	RPA
Hubbard: $U/t = 1.6$	π	AFQMC

[a] $S(\boldsymbol{q})$ is evaluated on a Slater-Jastrow wavefunction through variational Monte Carlo method. The Slater determinant is formed by the occupied π and σ orbitals.

[b] $S(\boldsymbol{q})$ is evaluated on a Slater-Jastrow wave function formed by only the occupied π orbitals. The Jastrow factor is the same one used in full graphene.

Our theoretical results were compared with experimental data from our previous IXS experiment [28]. The experiment was performed on single crystals of graphite and the response function of graphene is extracted from graphite according to the procedure described in Ref. [27].

Let us first consider the $S(\boldsymbol{q})$ results for *ab-initio* graphene, denoted by G in Fig. 2. For comparison, we have plotted $S(\boldsymbol{q})$ computed from a non-interacting Slater determinant of Kohn-Sham orbitals [G(Slater)], and that of a Slater-Jastrow wavefunction [G(S-J)]. Both RPA and DMC results are very close to the experimental IXS results, but there is a significant difference between the correlated calculations and the Slater determinant, as expected. The Slater-Jastrow result is indistinguishable from the DMC result. It thus appears that the experimental $S(\boldsymbol{q})$ is well reproduced by any of these three correlated techniques (RPA, S-J and DMC). Quantitatively, this change of $S(\boldsymbol{q})$ from the Slater determinant reflects a reduction of the Coulomb energy by 1.31(5) eV per electron.

Now consider the H, TB, Hubbard, and G_π models in Fig. 2, which only contain one electron per site (1e/site), in contrast to the four electrons per site (4e/site) of *ab-initio* graphene. Each of these models has a computed $S(\boldsymbol{q})$ quite close to the others. Therefore, if 1e/site is considered, $S(\boldsymbol{q})$ is about the same, regardless of the computational method and interaction. Also for 4e/site, $S(\boldsymbol{q})$ is about the same among these correlated calculations. We can thus assess the importance of the bonding σ electrons at different wavelengths by comparing the 1e/site curves to the 4e/site curves.

At the smallest values of q available to both the computational and experimental techniques, the 1e/site $S(\boldsymbol{q})$ differs from the 4e/site $S(\boldsymbol{q})$. We would expect those $S(\boldsymbol{q})$ to coincide for q small enough if it were the case that the σ electrons did not contribute to the long-range

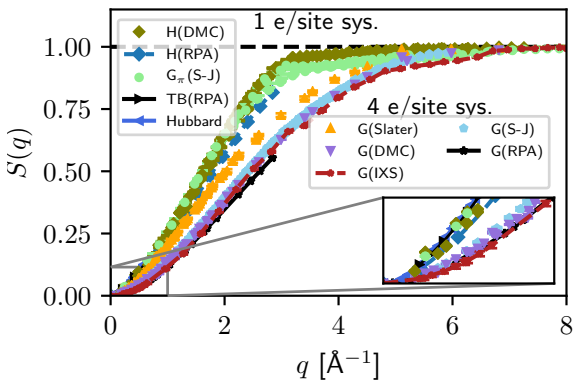

FIG. 2. $S(q)$ of different systems obtained through different methods. G: graphene; G$_\pi$: π electrons only graphene; H: hydrogen; TB: π-band tight-binding model with $1/r$ interactions; Hubbard: the Hubbard model with $U/t = 1.6$.

density density fluctuations. We thus conclude that the σ electrons contribute to the density-density fluctuations even for $q \sim 0.1 - 0.2$Å^{-1} and that $S(\boldsymbol{q})$ is accurately described by RPA, Slater-Jastrow, and DMC.

Now let us move to the dynamic response of graphene, $S(\boldsymbol{q}, \omega)$. Fig. 3(a) (b) and (c) shows the computed imaginary part of the response function $\chi(\boldsymbol{q}, \omega)$ of graphene in comparison with the IXS results at different q. RPA accurately reproduces the experimental data especially at small q. For example, at $q = 0.21$Å^{-1}, it accurately reproduces the two plasmon peaks [16, 18, 48–50]: (1)π plasmons from $\pi \to \pi^*$ interband transition; (2) $\sigma + \pi$ plasmons from $\sigma \to \pi^*$ and $\pi \to \sigma^*$ interband transition, denoted as ω_π and $\omega_{\sigma+\pi}$ respectively in Fig. 3(a). RPA is accurate even up to $q = 1.25$Å^{-1} [Fig. 3(b)]. It does become less accurate at large q (2.80Å^{-1}) [Fig. 3(c)], resulting an underestimate of $S(\boldsymbol{q})$ at short range for both graphene and the hydrogen system (see the small discrepancy between RPA and DMC curves in Fig. 2). Nevertheless, it appears that the long-range response is well-described by RPA calculations that include the σ electrons, at least to the limits of experimental resolution and potentially with small errors in the peak positions.

At small q, the $\pi+\sigma$ plasmons are inherently missing in the TB model and hydrogen system. This is why $S(\boldsymbol{q})$ in these two systems is larger than that in graphene (Fig. 2) If we exclude the $\pi + \sigma$ plasmons in the integration of Eq. (3) by setting the frequency cutoff to be 12eV, we would get an $S(\boldsymbol{q})$ similar to that of the TB model [see the G(IXS12) curve in Fig. 3(d)]. The frequency cutoff in our experimental data is $2,000$ eV which is high enough to include relevant excitations of valence electrons.

At large q, graphene and the hydrogen system have qualitatively different dynamic response [Fig. 3(b) and (c)]. This is mainly because the excitation of the bonding σ electron to high energy states in graphene, which is missing in the hydrogen system and other 1e/site systems, resulting a discrepancy of $S(\boldsymbol{q})$ between graphene and the hydrogen system at short range (see Fig. 2).

The π plasmon resonance peak ω_π of the TB model and hydrogen is 1 – 3 eV larger than that of graphene [Fig. 3(a) and (e)]. This indicates strong screening effects from the σ electrons in graphene which are not present in the TB model nor in the hydrogen system. The interaction from σ electron "renormalizes" the π plasmon resonance frequency.

Let us investigate the "renormalization" effect from σ electrons by reconsidering the dynamic response of TB model. The TB(RPA) curve in Fig. 3 was computed by assuming that the TB model is put in vacuum and that the π electrons interact with each other through a bare Coulomb interaction ($1/r$). Suppose it is in an environment of σ electrons, if we were within the RPA framework, we would have to include a background dielectric function $\kappa_\sigma(\boldsymbol{q})$ in the response function $\chi(\boldsymbol{q}, \omega)$ [28, 51],

$$\chi(\boldsymbol{q}, \omega) = \frac{\Pi_{\rm TB}(\boldsymbol{q}, \omega)}{\kappa_\sigma(\boldsymbol{q}) - V(\boldsymbol{q})\Pi_{\rm TB}(\boldsymbol{q}, \omega)}. \tag{4}$$

$\Pi_{\rm TB}(\boldsymbol{q}, \omega)$ is the polarization function in vacuum computed using the Lindhard function [51], and $V(\boldsymbol{q})$ is the Coulomb interaction in reciprocal space. A good estimation of κ_σ is [51, 52] [plotted in Fig. 3(f)] ,

$$\kappa_\sigma(\boldsymbol{q}) = \frac{\kappa_1 + 1 - (\kappa_1 - 1)e^{-qL}}{\kappa_1 + 1 + (\kappa_1 - 1)e^{-qL}}\kappa_1 \,. \tag{5}$$

$\kappa_1 \simeq 2.4$ is the dielectric constant of graphite, and $L = 2.8$Å is the effective thickness for a single layer graphene. The inclusion of κ_σ indeed reduces ω_π by about 1 – 2 eV [see the TB$_\sigma$(RPA) curve in Fig. 3(e)]. Thus, we confirmed that at the RPA level, the screening from σ electrons reduces the π plasmon resonance frequency.

The remaining discrepancy between TB$_\sigma$(RPA) and G(IXS) [or G(RPA)] is partially due to the deviation of tight-binding band dispersion from *ab-initio* graphene, since the π plasmon frequency ω_π is directly related to the $\pi \to \pi^*$ interband transition. This deviation can be seen from the calculated joint density of states (JDOS) shown in Fig. 4,

$$jdos(\omega) = \frac{1}{N_k}\sum_{\boldsymbol{k}} \delta(\epsilon_{\pi^*}(\boldsymbol{k}) - \epsilon_\pi(\boldsymbol{k}) - \omega)\,, \tag{6}$$

where $\epsilon_\pi(\boldsymbol{k})$ and $\epsilon_{\pi^*}(\boldsymbol{k})$ are the eigenvalues of π and π^* bands respectively, and N_k is the number of k points sampled in the first Brillouin zone. Because of the van Hove singularity at the M point, there is a peak located near $\epsilon_{\pi^*}(M) - \epsilon_\pi(M)$. The $\pi \to \pi^*$ transition energy at M point is 5.4 eV for the tight-binding model, 4.2 eV for *ab-initio* graphene, and 4.0 eV for hydrogen (see Fig. 1). The peak shifts towards high energy from graphene to the tight-binding model, which causes a difference of ω_π by about 1 eV.

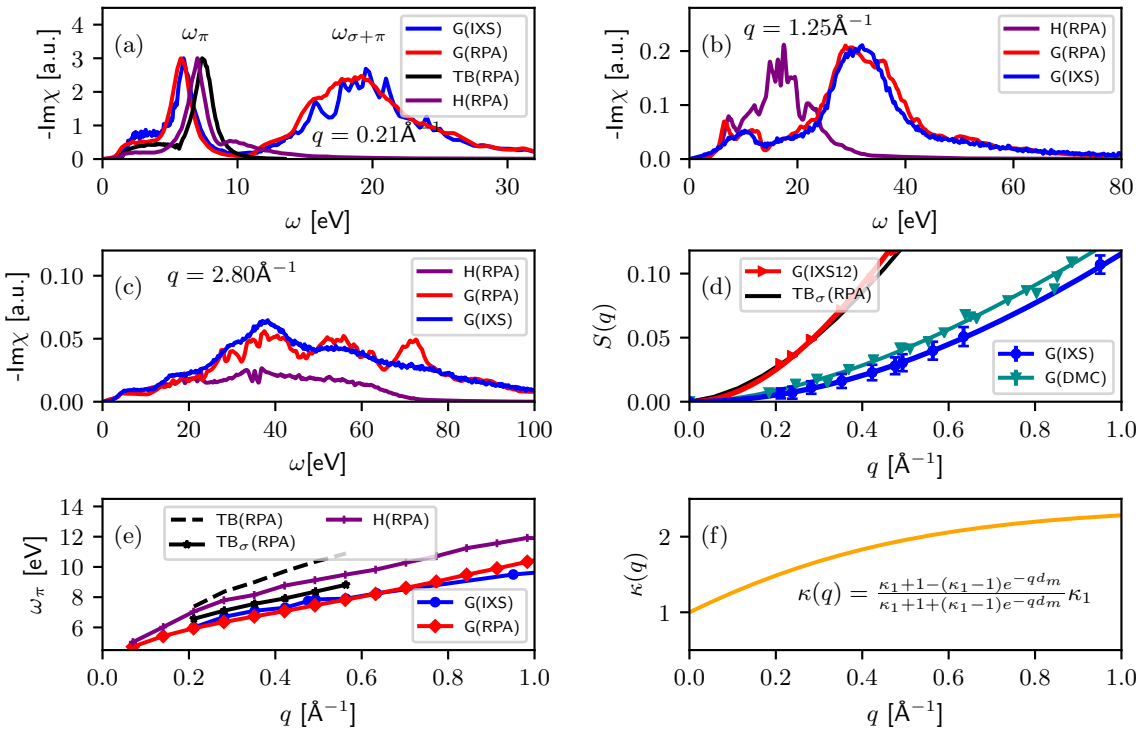

FIG. 3. Effect of σ electrons. (a) (b), and (c): imaginary part of the response function $\chi(q,\omega)$ of graphene (G), the hydrogen system (H) and the tight-binding model (TB) from either X-ray experiment or RPA calculations at $q = 0.21, 1.25,$ and 2.80Å^{-1}. (d) $S(q)$ of graphene from integration of $S(q,\omega)$ with different upper frequency limit ω_c: G(IXS) – 2,000 eV; G(IXS12) – 12 eV. (e) $\pi \to \pi^*$ plasmon dispersion. (f) effective screening function from σ electrons.

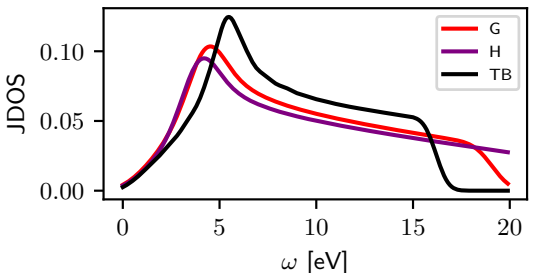

FIG. 4. Joint density of states of graphene (G), hydrogen (H), and tight-binding model (TB) computed from PBE band structure and tight-binding band structure.

Now consider the screening effect from the σ electrons at different wavelengths. This can be seen from the difference between ω_π of graphene and the hydrogen system, since the band structure deviation between the two systems is small up to the energy scale of ω_π [see the JDOS in Fig. 4] and the difference of ω_π is mainly caused by the screening from σ electrons in graphene. This difference of ω_π between the two systems decreases as $q \to 0$ [Fig. 3(e)]. In the limit as $q \to 0$, the screening from the σ electrons goes to zero, which is also reflected in κ_σ: $\kappa_\sigma \to 1$ if $q \to 0$ [Fig. 3(f)]. However, even at the lowest momentum that the IXS experiment has access to ($q = 0.21$Å^{-1}) [28], the screening effect is not small [$\kappa_\sigma(q) \simeq 1.5$]. It causes a shift of ω_π by 0.8 eV, which is comparable to estimations of excitonic effects [27–29]. If it is desired to isolate the π electrons from the σ electron screening, one would have to reach the regime of $q \ll 0.21$Å^{-1}. For example, at $q = 0.07$ Å^{-1}, the shift reduces to 0.25 eV [Fig. 3(e)]. For this reason, π-only models are accurate at small q regime, for example, in describing the renormalization of the quasiparticle dispersion near Dirac point [10, 12] and the infrared dispersion of the intraband plasmon in doped graphene [9]. However, without including the σ electron screening, π-only models even incorrectly predict an insulating graphene in vacuum [52–55].

In conclusion, using the first-principles quantum Monte Carlo approach and the random phase approximation with DFT as the reference, we are able to describe the electron correlations in graphene accurately and reproduce the X-ray data very well for all q available, provided that the σ electrons are included in the calculations. It is clear that the σ electrons are important for the interpretation of IXS data even at ranges up to around 80 Å. For very small values of q, the π-only model is accurate, but the experimental data does not reach those regimes.

The σ electrons impact the calculation in two impor-

tant ways. First, at long wavelength, the σ electrons respond through $\pi + \sigma$ plasmons which causes graphene to have an $S(q)$ different from tight-binding model and hydrogen. The screening from the σ electrons reduces the π plasmon resonance frequency by about $1 - 2$ eV which is comparable to other effects such as excitons [29] that will cause similar shifts. Second, with the presence of σ electrons, the band structure of graphene deviates from a π-orbital tight-binding model, which further modifies the spectrum. These effects are observable even at $q = 0.21\text{Å}^{-1}$, the lowest momentum that current X-ray experiments can access.

This study shows that unprecedented detail into electron correlations can be obtained both from the experimental and theoretical points of view, even for a system like graphene which has an unusual low-energy band structure. Without adjustable parameters, we have demonstrated the direct correspondence between density-density fluctuations measured by inelastic X-ray experiments and that calculated by theory. If the effects of all valence electrons in graphene are carefully taken into account, it appears possible to account for most of the correlations in graphene using standard techniques. Careful consideration of valence electrons might also be needed to describe correlated physics of similar systems like Weyl semimetals and surface states of topological insulators.

The authors would like to thank Hitesh Changlani for helpful discussions in performing AFQMC calculations for Hubbard model, André Schleife for useful discussions, Bruno Uchoa for inspiring the work, and Duncan J. Mowbray for providing details about RPA calculations for graphene. This material is based upon work supported by the U.S. Department of Energy, Office of Science, Office of Advanced Scientific Computing Research, Scientific Discovery through Advanced Computing (SciDAC) program under Award Number FG02-12ER46875. P.A. acknowledges support from DOE grant # DE-FG02-06ER46285. Computational resources were provided by the DOE INCITE SuperMatSim/PhotoSuper programs and the Taub campus cluster at the University of Illinois at Urbana-Champaign.

* lkwagner@illinois.edu

[1] P. R. Wallace, Physical Review **71**, 622 (1947).
[2] K. S. Novoselov, A. K. Geim, S. V. Morozov, D. Jiang, Y. Zhang, S. V. Dubonos, I. V. Grigorieva, and A. A. Firsov, Science **306**, 666 (2004).
[3] K. S. Novoselov, A. K. Geim, S. V. Morozov, D. Jiang, M. I. Katsnelson, I. V. Grigorieva, S. V. Dubonos, and A. A. Firsov, Nature **438**, 197 (2005).
[4] M. I. Katsnelson, K. S. Novoselov, and A. K. Geim, Nat Phys **2**, 620 (2006).
[5] A. K. Geim and K. S. Novoselov, Nature Materials **6**, 183 (2007).
[6] K. S. Novoselov, Z. Jiang, Y. Zhang, S. V. Morozov, H. L. Stormer, U. Zeitler, J. C. Maan, G. S. Boebinger, P. Kim, and A. K. Geim, science **315**, 1379 (2007).
[7] A. H. Castro Neto, F. Guinea, N. M. R. Peres, K. S. Novoselov, and A. K. Geim, Reviews of Modern Physics **81**, 109 (2009).
[8] A. H. Castro Neto, F. Guinea, N. M. R. Peres, K. S. Novoselov, and A. K. Geim, Reviews of Modern Physics **81**, 109 (2009).
[9] V. N. Kotov, B. Uchoa, V. M. Pereira, F. Guinea, and A. H. Castro Neto, Reviews of Modern Physics **84**, 1067 (2012).
[10] J. Gonzalez, F. Guinea, and M. A. H. Vozmediano, Physical Review Letters **77**, 3589 (1996).
[11] C. D. Spataru, M. A. Cazalilla, A. Rubio, L. X. Benedict, P. M. Echenique, and S. G. Louie, Physical Review Letters **87**, 246405 (2001).
[12] S. Das Sarma, E. H. Hwang, and W.-K. Tse, Physical Review B **75**, 121406 (2007).
[13] D. C. Elias, R. V. Gorbachev, A. S. Mayorov, S. V. Morozov, A. A. Zhukov, P. Blake, L. A. Ponomarenko, I. V. Grigorieva, K. S. Novoselov, F. Guinea, and A. K. Geim, Nature Physics **7**, 701 (2011).
[14] K. I. Bolotin, F. Ghahari, M. D. Shulman, H. L. Stormer, and P. Kim, Nature **462**, 196 (2009).
[15] A. Bostwick, F. Speck, T. Seyller, K. Horn, M. Polini, R. Asgari, A. H. MacDonald, and E. Rotenberg, Science **328**, 999 (2010).
[16] F. Bassani and G. P. Parravicini, Il Nuovo Cimento B Series 10 **50**, 95 (1967).
[17] A. G. Marinopoulos, L. Reining, A. Rubio, and V. Olevano, Physical Review B **69**, 245419 (2004).
[18] T. Eberlein, U. Bangert, R. R. Nair, R. Jones, M. Gass, A. L. Bleloch, K. S. Novoselov, A. Geim, and P. R. Briddon, Physical Review B **77**, 233406 (2008).
[19] D. Pines, *The Many-body Problem* (Basic Books, 1997).
[20] S. Murakami, New Journal of Physics **9**, 356 (2007).
[21] S.-M. Huang, S.-Y. Xu, I. Belopolski, C.-C. Lee, G. Chang, B. Wang, N. Alidoust, G. Bian, M. Neupane, C. Zhang, S. Jia, A. Bansil, H. Lin, and M. Z. Hasan, Nature Communications **6**, 7373 (2015).
[22] S.-Y. Xu, I. Belopolski, N. Alidoust, M. Neupane, G. Bian, C. Zhang, R. Sankar, G. Chang, Z. Yuan, C.-C. Lee, S.-M. Huang, H. Zheng, J. Ma, D. S. Sanchez, B. Wang, A. Bansil, F. Chou, P. P. Shibayev, H. Lin, S. Jia, and M. Z. Hasan, Science **349**, 613 (2015).
[23] B. Q. Lv, H. M. Weng, B. B. Fu, X. P. Wang, H. Miao, J. Ma, P. Richard, X. C. Huang, L. X. Zhao, G. F. Chen, Z. Fang, X. Dai, T. Qian, and H. Ding, Phys. Rev. X **5**, 031013 (2015).
[24] M. Z. Hasan and C. L. Kane, Rev. Mod. Phys. **82**, 3045 (2010).
[25] X.-L. Qi and S.-C. Zhang, Rev. Mod. Phys. **83**, 1057 (2011).
[26] Y. Ando, Journal of the Physical Society of Japan **82**, 102001 (2013).
[27] J. P. Reed, B. Uchoa, Y. I. Joe, Y. Gan, D. Casa, E. Fradkin, and P. Abbamonte, Science **330**, 805 (2010).
[28] Y. Gan, G. A. de la Peña, A. Kogar, B. Uchoa, D. Casa, T. Gog, E. Fradkin, and P. Abbamonte, Phys. Rev. B **93**, 195150 (2016).
[29] P. E. Trevisanutto, M. Holzmann, M. Cote, and V. Olevano, Physical Review B **81**, 121405 (2010).
[30] W. M. C. Foulkes, L. Mitas, R. J. Needs, and G. Rajagopal, Reviews of Modern Physics **73**, 33 (2001).

[31] J. Kolorenc, S. Hu, and L. Mitas, Physical Review B **82**, 115108 (2010).

[32] G. G. Spink, R. J. Needs, and N. D. Drummond, Physical Review B **88**, 085121 (2013).

[33] L. K. Wagner, M. Bajdich, and L. Mitas, Journal of Computational Physics **228**, 3390 (2009).

[34] L. K. Wagner and L. Mitas, The Journal of Chemical Physics **126**, 034105 (2007).

[35] N. D. Drummond and R. J. Needs, Physical Review B **88**, 035133 (2013).

[36] L. K. Wagner and P. Abbamonte, Physical Review B **90**, 125129 (2014).

[37] H. Zheng and L. K. Wagner, Physical Review Letters **114**, 176401 (2015).

[38] L. K. Wagner, Physical Review B **92**, 161116 (2015).

[39] S. Chiesa, D. M. Ceperley, R. M. Martin, and M. Holzmann, Physical Review Letters **97**, 076404 (2006).

[40] D. J. Mowbray, physica status solidi (b) **251**, 2509 (2014).

[41] R. Dovesi , V.R. Saunders , C. Roetti, R. Orlando, C. M. Zicovich-Wilson, F. Pascale, B. Civalleri, K. Doll, N.M. Harrison, I.J. Bush, Ph. DArco, M. Llunell, "User's manual of CRYSTAL,".

[42] J. P. Perdew, K. Burke, and M. Ernzerhof, Physical Review Letters **77**, 3865 (1996).

[43] M. Burkatzki, C. Filippi, and M. Dolg, The Journal of Chemical Physics **126**, 234105 (2007).

[44] M. Burkatzki, C. Filippi, and M. Dolg, The Journal of Chemical Physics **129**, 164115 (2008).

[45] J. J. Mortensen, L. B. Hansen, and K. W. Jacobsen, Physical Review B **71**, 035109 (2005).

[46] J. Yan, J. J. Mortensen, K. W. Jacobsen, and K. S. Thygesen, Phys. Rev. B **83**, 245122 (2011).

[47] C. N. Varney, C.-R. Lee, Z. J. Bai, S. Chiesa, M. Jarrell, and R. T. Scalettar, Physical Review B **80**, 075116 (2009).

[48] R. Ahuja, S. Auluck, J. M. Wills, M. Alouani, B. Johansson, and O. Eriksson, Physical Review B **55**, 4999 (1997).

[49] P. E. Trevisanutto, C. Giorgetti, L. Reining, M. Ladisa, and V. Olevano, Physical Review Letters **101**, 226405 (2008).

[50] C. Kramberger, R. Hambach, C. Giorgetti, M. H. Rümmeli, M. Knupfer, J. Fink, B. Büchner, L. Reining, E. Einarsson, S. Maruyama, F. Sottile, K. Hannewald, V. Olevano, A. G. Marinopoulos, and T. Pichler, Phys. Rev. Lett. **100**, 196803 (2008).

[51] S. Yuan, R. Roldan, and M. I. Katsnelson, Physical Review B **84**, 035439 (2011).

[52] T. O. Wehling, E. Şaşıoğlu, C. Friedrich, A. I. Lichtenstein, M. I. Katsnelson, and S. Blügel, Phys. Rev. Lett. **106**, 236805 (2011).

[53] J. E. Drut and T. A. Lahde, Physical Review Letters **102**, 026802 (2009).

[54] M. V. Ulybyshev, P. V. Buividovich, M. I. Katsnelson, and M. I. Polikarpov, Physical Review Letters **111**, 056801 (2013).

[55] D. Smith and L. von Smekal, Physical Review B **89**, 195429 (2014).